

Impact of Two Lung Elastance Identification Methods on Pulmonary Mechanics Prediction

Qianhui Sun*, J. Geoffrey Chase*, Cong Zhou**, Merryn H. Tawhai***, Jennifer L. Knopp*, Knut Möller****, Geoffrey M. Shaw*****

* *Department of Mechanical Engineering; Dept of Mechanical Eng, Centre for Bio-Engineering, University of Canterbury, Christchurch, New Zealand (e-mail: qianhui.sun@pg.canterbury.ac.nz; geoff.chase@canterbury.ac.nz; cong.zhou@nwpw.edu.cn; jennifer.knopp@canterbury.ac.nz)*

** *School of Civil Aviation, Northwestern Polytechnical University, China*

*** *Auckland Bioengineering Institute, The University of Auckland, Auckland, New Zealand (e-mail: m.tawhai@auckland.ac.nz)*

**** *Institute for Technical Medicine, Furtwangen University, Villingen-Schwenningen, Germany (e-mail: Knut.Moeller@hs-furtwangen.de)*

***** *Department of Intensive Care, Christchurch Hospital, Christchurch, New Zealand (e-mail: geoff.shaw@cdhb.health.nz)*

Abstract: Positive-end-expiratory-pressure (PEEP) have proved effective in recruiting lung volume and keeping alveoli open. However, there is no standard means to find an optimal patient-specific PEEP, creating variability in care and outcomes. There is thus a need for personalized approaches to find the best PEEP and optimise care. This research extends a well-validated virtual patient model with a newly proposed function to predict lung distension, while the impact on outcome of two different elastance identification strategies are discussed and compared. A prior studied and effective exponential basis function set is used as the general model, while elastance are identified using overlapped and separate methods, respectively. In this approach, model with overlapped elastance identification and proposed distension function yields an absolute median peak inspiratory pressure (PIP) prediction error of 1.50cmH₂O for 623 prediction cases. Comparison between clinically measurement and model prediction for PIP yields R²=0.90 across 623 predictions in total, while R²=0.87 with separate elastance identification. Furthermore, both elastance identification methods are an improvement compared to predictions without proposed distension function (R²=0.82). Validation is fulfilled with 18 volume controlled ventilation patients respiratory data at 7 different baseline PEEP levels (0-12cmH₂O) with a maximal PEEP prediction interval of 12cmH₂O. Overall, the results demonstrate the impact of elastance identification methods, as well as the potential and significance for accurately capturing distension mechanics, which thus providing guidance for clinical care and insights for predictive lung mechanics modelling.

Copyright © 2021 The Authors. This is an open access article under the CC BY-NC-ND license (<https://creativecommons.org/licenses/by-nc-nd/4.0/>)

Keywords: Virtual Patient; Digital Twin; Mechanical ventilation; Critical Care; Basis function; Prediction; Elastance identification; Lung distension; VILI; Pressure-Volume loop.

1. INTRODUCTION

Ventilator induced lung injury (VILI) is one of the risks of suboptimal mechanical ventilation (MV) care, increasing morbidity and mortality (Carney et al., 2005; Pavone et al., 2007). This risk increases in positive-end-expiratory-pressure (PEEP) titration which is capable to keep alveoli open and ensure adequate oxygenation for respiratory failure patients (Briel et al., 2010).

Variability in care and risk occurred since no standard method in determining the optimal personalized PEEP level for patients (Chase et al., 2018; Chiew et al., 2011; Kim et al., 2020). Although model-based approaches are one means to personalize care (Chase et al., 2018), and assess lung mechanics (Damanhuri et al., 2016; Sundaresan & Chase, 2012; Sundaresan et al., 2011), very few is able to predict pulmonary mechanics at a new PEEP level with limited

bedside available information (Morton et al., 2019a; Morton et al., 2019b; Morton et al., 2020; Zhou et al., 2021), which is more likely the situation occurred in the intensive care unit. Thus, an accurate, predictive lung mechanics model would help clinicians select and test MV settings with lower risks.

Patient-specific basis functions have been proposed for biomedical simulation and prediction and are capable to offer novel, model-based insight into physiological mechanics (Langdon et al., 2018; Morton et al., 2019b; Morton et al., 2020). A nonlinear, physiologically-relevant hysteresis loop model (HLM) using an exponential basis function set accurately predicted the evolution of lung mechanics as MV settings changed for both VCV and pressure controlled ventilation (Zhou et al., 2021), but did not capture distension in VCV, which is considered as one of the most important factors related to VILI (Galiatsou et al., 2006).

This research discussed two different elastance identification methods influence on model prediction outcome, while an added personalized basis function is proposed to capture lung distension as an extension of the model in (Zhou et al., 2021). Overall, better prediction outcome is achieved with overlapped elastance identification and proposed distension function in this approach, while novel insights for distension prediction and elastance modelling strategy are offered.

2. METHODS

2.1 HLM lung mechanics model

The dynamic equation of motion for the HLM lung mechanics model is defined (Zhou et al., 2021):

$$\ddot{V} + R\dot{V} + K_e V + K_{h1}V_{h1} + K_{h2}V_{h2} = f_V(t) + PEEP \quad (1)$$

where V is the volume of air delivered to the lungs, V_{h1} and V_{h2} are hysteretic volume response during inspiration and expiration, respectively, K_e represents the alveolar recruitment elastance, named $k2$ in this approach, K_{h1} and K_{h2} , are determined by two nonlinear hysteretic springs for alveolar hysteresis elastance during inspiration and expiration, respectively, R is the airway resistance, PEEP is the positive end-expiratory pressure, and $f_V(t)$ is the steady-state input force. Detailed formulations for calculating each parameter can be found in (Zhou et al., 2021).

2.2 P-V loop identification

At any baseline $PEEP_i$ ($i = 1$), the hysteresis loop analysis method (HLA) can identify elastance values. Expiration is not identified and discussed in this study focusing on peak inspiratory pressure (PIP) prediction and distension during inspiration. For inspiration, the half cycle is first divided into 2 segments, with $k1$ for the first short segment and $k2$, $k2end$ for the longer segment ending at the peak inspiratory pressure. Two previously presented $k2$ and $k2end$ identification methods are applied.

Method 1 ($k2_{op}$): An overall $k2$ is first identified across the long segment. Then the segment is assessed again to find a potential, increased stiffness (reduced compliance) third segment, $k2end$, which will use the newly proposed basis function prediction procedure to capture over-distension as PEEP rises, as shown in Figure 1 (a).

Method 2 ($k2_{sp}$): $k2$ and $k2end$ are identified and separated with the breakpoint at the upper inflection point, which is automatically identified by HLA (Zhou & Chase, 2020; Zhou et al., 2015), as shown in Figure 1 (b).

Since at lower PEEP levels the overdistension is less likely to be observed yielding little or no difference between $k2$ and $k2end$ for both two methods, the prediction performance is assumed to have larger difference if a flattening curve is observed as pressure approaches PIP (usually at higher PEEP levels). Note the two identification methods will only have influence in the value of $k2_1$ while $k2end$ is exactly the same. Thus, three prediction combinations are possible in this study comprising: $k2_{op}$ without any $k2end$; $k2_{sp}$ with $k2end$ (Method 2); and $k2_{op}$ with $k2end$ (Method 1).

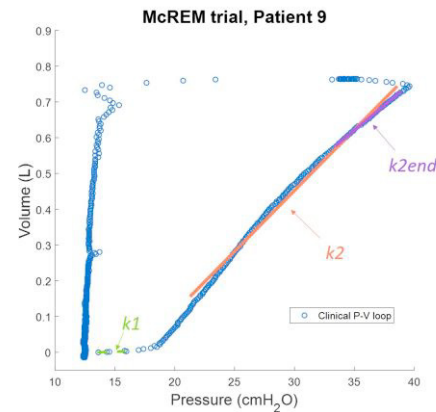
2.3 Basis functions for elastance prediction

After HLA identification of a single breath at any PEEP, an exponential basis function set used in prior studies (Lauer et al., 2017; Morton et al., 2018; Zhou et al., 2021), is used to predict the evolution of recruitment elastance (for both $k2_{op}$ and $k2_{sp}$) at higher PEEP ($i > 1$). It assumes elastance has a bowl shape across PEEP (Zhou et al., 2021) and is defined:

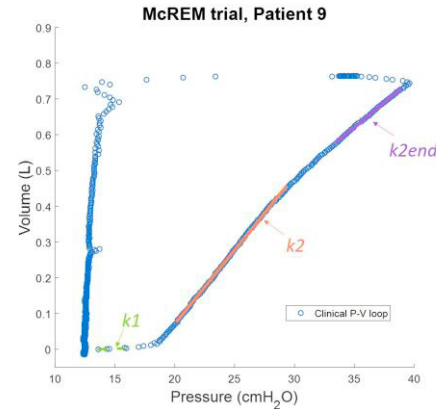
$$k2_i = \left(\frac{PEEP_i}{k1} + \frac{k2_1}{k1} * e^{b * \frac{PEEP_i}{k1}} \right) * k1 \quad (2)$$

$$b = \frac{k1}{PEEP_1} * \log \frac{k2_1 - PEEP_1}{k2_1} \quad (3)$$

Where b is the exponential rate of recruitment, $k1$ and $k2_1$ are the identified values via HLA from baseline PEEP, and $PEEP_i$ is the predicted PEEP level.



(a) Elastance identification with overlapped $k2$ using Method 1



(b) Elastance identification with separate $k2$ identified simultaneously using Method 2

Figure 1 Examples of HLA identification for a measured clinical P-V loop at a baseline PEEP = 12cmH₂O for Patient 9, (a) with separate $k2_{sp}$ and (b) overlapped $k2_{op}$ identification from $k2end$.

At the same time, the evolution of distension at higher PEEP levels ($k2end_i$, $i > 1$) is also predicted. In this approach, end expiratory volume ($EELV_1$) and expiratory tidal volume ($PIV_1 - EELV_1$, with PIV_1 peak inspiratory volume) identified at baseline PEEP are assumed to interact with predicted $k2_i$ to predict $k2end$ distension elastance evolution with PEEP. A new basis function is thus proposed to capture and predict the evolution of over-distension in $k2end$ for HLM modelling:

$$k2end_i = \left(\frac{PEEP_i}{k2_i} + \frac{k2end_1}{k2_1} * (\theta1 + \theta2^2) \right) * k2_i \quad (4)$$

$$\theta1 = \frac{k2end_1 - PEEP_1}{k2end_1} \quad (5)$$

$$\theta2 = \Delta PEEP * \frac{EELV_1}{PIV_1 - EELV_1} \quad (6)$$

Where $\Delta PEEP = PEEP_i - PEEP_1$. Figure 2 shows a sketch of basis function terms over PEEP for $k2end$ evolution.

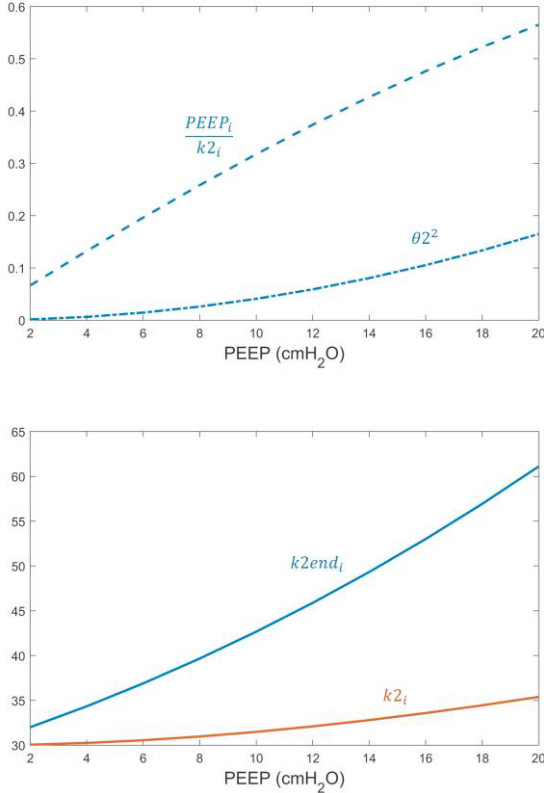


Figure 2 Upper panel illustrates the contribution of each term and how they change over PEEP for $k2end$ prediction in (4)-(6), while lower panel presents the yielding $k2end_i$ with predicted $k2_i$.

2.4 Patient data

Ventilation data from 18 ventilated ICU patients from the McREM trial (Stahl et al., 2006) is used to validate the basis functions and methods proposed. All patients were fully sedated and intubated under invasive VCV. The McREM trial was conducted across eight German university ICUs from September 2000 to February 2002 (Stahl et al., 2006). One incremental staircase recruitment maneuver (RM) with $\Delta PEEP = 2\text{cmH}_2\text{O}/\text{step}$ was performed for each patient starting at $0\text{cmH}_2\text{O}$. The prediction procedure is applied for higher PEEP levels ($i = 2, \dots, 7$) after identification at baseline PEEP ($i = 1$). To test the robustness and generality of the HLM model and basis function sets, prediction tests are applied across a range of baseline PEEP = 0, 2, 4, 6, 8, 10, and $12\text{cmH}_2\text{O}$ with a further 6 prediction steps ($2\text{cmH}_2\text{O}$ interval) from each baseline level, yielding a maximum value for $\Delta PEEP = 2 \times 6 \text{ steps} = 12\text{cmH}_2\text{O}$. There are thus a total of 623 predictions across the 7 baseline PEEP test groups and

patients. Demographics for the patients can be found in (Zhou et al., 2021) due to space limitations.

3. RESULTS

The cumulative distribution function (CDF) plots are presented in Figure 3 (623 predictions) showing the error reductions in PIP prediction obtained using the proposed $k2end$ function and its evolution. Moreover, an overall prediction accuracy improvement occurred in prediction group with a combination of $k2_{op}$ identification and $k2end$ prediction, with the lowest median error of $1.50\text{cmH}_2\text{O}$. Assessing only clinically relevant $\Delta PEEP = 2\text{-}6\text{cmH}_2\text{O}$ (1-3 prediction steps), Table 1 shows the PIP prediction outcome for $\Delta PEEP = 2\text{-}12\text{cmH}_2\text{O}$ and $\Delta PEEP = 2\text{-}6\text{cmH}_2\text{O}$ across 3 combinations, where $k2_{op}$ with $k2end$ still yields the highest accuracy.

Table 1 - PIP prediction errors presented in yielding R^2 , median error, and IQR range (cmH_2O) for 1-6 prediction steps further ($\Delta PEEP = 2\text{-}12\text{cmH}_2\text{O}$) and 1-3 prediction steps further ($\Delta PEEP = 2\text{-}6\text{cmH}_2\text{O}$).

PIP prediction outcome	Without $k2end$	With $k2end$	
		$k2_{sp}$	$k2_{op}$
1-6 steps			
623 prediction cases			
R^2	0.82	0.87	0.90
90 th % error	4.76	4.43	3.95
median	1.80	1.76	1.50
[IQR]	[0.90 3.14]	[0.78 3.11]	[0.69 2.55]
1-3 steps			
356 prediction cases			
R^2	0.88	0.90	0.93
90 th % error	3.84	3.56	2.93
median	1.47	1.38	1.19
[IQR]	[0.75 2.56]	[0.58 2.54]	[0.48 1.99]

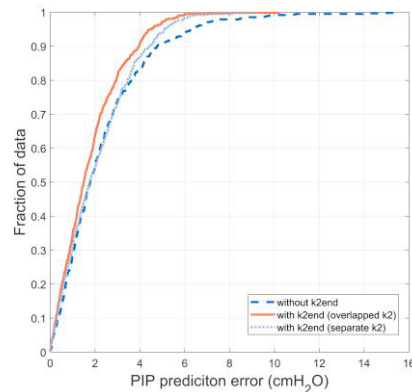


Figure 3 The CDF plot for absolute PIP prediction errors (dash line) without $k2end$, (dotted line) $k2_{sp}$, and (solid line) $k2_{op}$ with $k2end$ function for for 623 cases ($\Delta PEEP = 2\text{-}12\text{cmH}_2\text{O}$).

Boxplots for absolute PIP prediction errors for the 3 combinations of elastances are presented in Figure 4. Using the $k2end$ function results in fewer and smaller outliers in all 7

baseline PEEP levels, with the lowest median error of 1.50cmH₂O, in predictions with $k2_{op}$ and $k2_{end}$. Overall, 90% of PIP prediction errors are within 4.76cmH₂O, 4.42cmH₂O, and 3.95cmH₂O in sequence. Figures 3-4 show the novel added $k2_{end}$ prediction presented captures possible over-distension and barotrauma in VCV patients, especially with $k2_{op}$ identification.

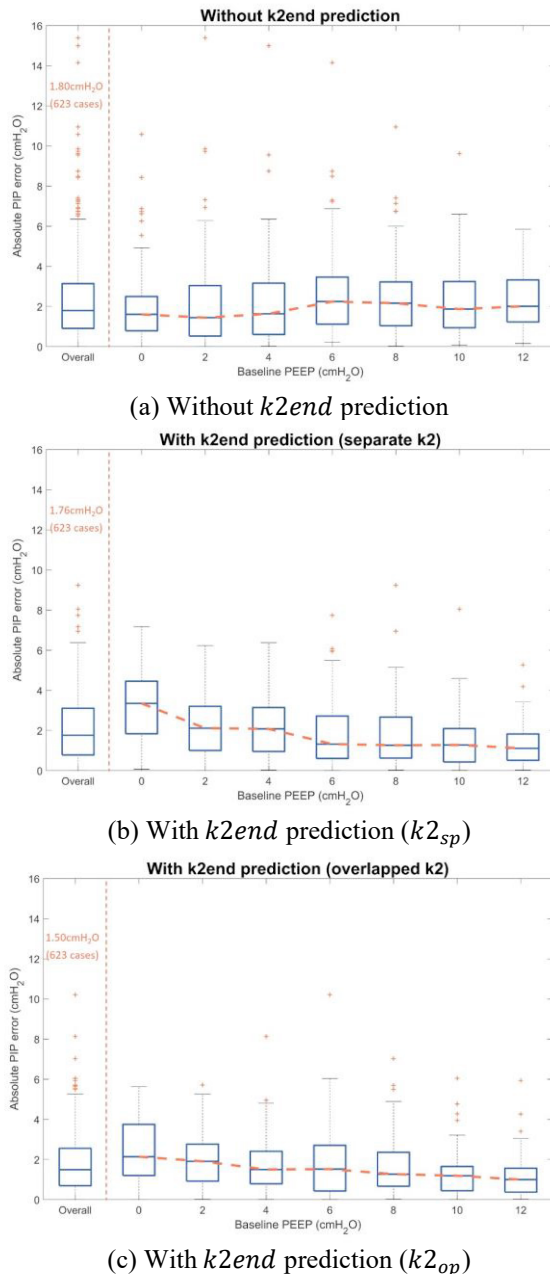


Figure 4 Boxplots for PIP prediction errors over 7 baseline PEEPs for predictions (a) without $k2_{end}$, (b) $k2_{sp}$ with $k2_{end}$, and (c) $k2_{op}$ with $k2_{end}$.

4. DISCUSSION

As in prior works (Jonson et al., 1999; Sundaresan & Chase, 2012; Zhou et al., 2021), the segment of the P-V loop between the lower inflection point (LIP) and upper inflection point (UIP) is treated as linear, while the segment above UIP until the end of inspiration ($k2_{end}$) is specially identified as a

separate linear segment in this approach which is treated as curvilinear and constant over PEEP in (Jonson et al., 1999) and not considered in other works (Sun et al., 2020; Sundaresan & Chase, 2012). UIP is considered as an upper limit before distension has been approximated in clinical studies (Kárason et al., 2001; Maggiore et al., 2003; Stenqvist & Odenstedt, 2007), but this study is the first model-based effort to quantify and to predict distension. Although two different $k2$ and $k2_{end}$ identification methods have been studied in (Fisher et al., 1988; Jonson et al., 1999) to simulate lung mechanics and discussed the correspondence with over-distension. Neither was model-based and neither included prediction or compared the efficiency for these two methods.

After identification, the evolution of $k2$ and $k2_{end}$, are predicted using (2)-(6), where prediction accuracy is the key to clinical utility in guiding MV (Chase et al., 2018; Morton et al., 2019a). Identifying and predicting $k2_{end}$ is a novel model capability and a key feature of this approach as it directly captures potential barotrauma in VCV and over-distension and thus the risk of VILI. The amount of over-distension is a critical factor in VCV care, as recruiting more lung when over-distension occurs also means healthy lung units may be damaged (Gomez-Laberge et al., 2012; Vieira et al., 1998). Even with a similar rate of $k2$ changes from baseline PEEP to a much higher PEEP level, the amount of distension can be distinct from patient to patient. For example, while the ratio of the change in $k2_{op}$ is both ~ 1.60 for Patients 9 and 14 (both from prediction at PEEP = 18 from 6cmH₂O), the amount of distension over pressure can be distinct from 2.75cmH₂O to 0.03cmH₂O, respectively. Thus, distension and $k2_{end}$ can be even more patient-specific than the recruitment elastance, $k2$, but provide significant new lung mechanics insight to optimise VCV, while also helping reduce the risk of VILI. Since $k2_{end}$ evolution is assumed to be correlated with $k2$ in this approach, the $k2$ identification procedure choice is also of value.

Some lung imaging methods, such as computed tomography scans, are able to identify alveoli recruitment and distension during clinical treatment (Cereda et al., 2013; Fumagalli et al., 2019). However, they are typically invasive and costly. Equally, regardless of the availability and the requirement of additional devices, none of these imaging methods enable prediction of over-distension based on images at a single PEEP level, reinforcing the potential clinical utility of a model-based digital twin or virtual patient approach (Chase et al., 2018) as presented here.

Overall, PIP prediction errors with proposed $k2_{end}$ function are improved with less outliers for $k2_{sp}$ combination and overall lower errors for $k2_{op}$ combination, as shown in Figures 3-4. Furthermore, the median error tends to be higher as baseline PEEP increases in predictions without $k2_{end}$, while the tendency is decrease in predictions with proposed $k2_{end}$ function, whether $k2_{sp}$ or $k2_{op}$. Although the overall error range is similar in predictions without $k2_{end}$ and $k2_{sp}$ with $k2_{end}$, overshooting bias, which can lead to a more conservative clinical decision, is 25.4% and 68.7%, respectively (60.8% in $k2_{op}$ predictions). Thus, added $k2_{end}$ function still shows a clinical relevant benefit.

Figure 4 shows using the same prediction procedure with $k2_{end}$ prediction, $k2_{sp}$ prediction accuracy at baseline PEEP = 4-6cmH₂O slightly exceeds that of $k2_{op}$. However, the large errors in $k2_{op}$ and $k2_{sp}$ prediction all occurred in Patient 16, and at higher Δ PEEP changes. Patient 16 is the only patient in the McREM trial with an extremely low P/F ratio = 75, while all others are all above 140. A P/F ratio lower than 100 can be the indicator of very severe ARDS and is a predictor of mortality (Adams et al., 2020; Force*, 2012). Thus, this patient has much worse pulmonary condition compared to the other 17 McREM patients, many of whom also meet broad less severe ARDS definitions (The ARDS Definition Task Force, 2012). If this patient is excluded, the 90th error falls to 3.88cmH₂O and 4.34cmH₂O, respectively. For prediction under Δ PEEP = 2-6cmH₂O, it decreases to 2.87cmH₂O and 3.46cmH₂O.

The newly presented $k2_{end}$ function and prediction of its evolution as PEEP changes significantly improve the overall prediction performance for both $k2$ identification methods, even for a patient with much worse lung condition (P/F<100), which shows the importance of including a separate $k2_{end}$ prediction to capture over distension, and offers a promising, clinically useful prediction method, particularly at higher PEEP levels where peak pressures will be high enough for distension to be likely.

Moreover, it presents the difference between two $k2$ identification methods. While the $k2_{sp}$ might be more intuitive, the overlapped $k2_{op}$ yields an overall better performance in this approach, which may have more mathematical significance for modelling. However, these results may limit to the prediction function efficiency, patient number, MV modes, and other possible factors.

Overall, prediction performance accessed across 18 ventilated patients at a wide range of different baseline PEEP levels (from 0 to 12cmH₂O) with Δ PEEP prediction intervals up to 12cmH₂O. While being effective and reducing modelling effort, the overall outcome shows the physiological relevant basis function sets offer the possibility for accurate and simpler lung mechanics prediction, especially over clinically realistic Δ PEEP=2-6cmH₂O intervals.

5. CONCLUSIONS

In conclusion, this study presents an extended and more accurate virtual patient model for volume controlled ventilation, including novel terms to capture and predict the clinically important risk of over-distension and thus the risk of VILI. The yielding difference by elastance identification methods for studied pilot trial are also discussed. It presents the promising ability of physiologically relevant basis functions for lung mechanics prediction at a single baseline PEEP breath and novel insights for elastance identification strategy. More clinical data are still required to further validate this MV virtual patient modelling methodology to personalise and optimise MV treatment.

6. ACKNOWLEDGEMENTS

This work was supported by the NZ Tertiary Education Commission (TEC) fund MedTech CoRE (Centre of Research Excellence; #3705718) and the NZ National Science Challenge 7, Science for Technology and Innovation (2019-S3-CRS). The authors also acknowledge support from the EU H2020 R&I programme (MSCA-RISE-2019 call) under grant agreement #872488 — DCPM.

REFERENCES

- Adams, JY, Rogers, AJ, Schuler, A, Marelich, GP, Fresco, JM, Taylor, SL, Riedl, AW, Baker, JM, Escobar, GJ & Liu, VX 2020, 'Association Between Peripheral Blood Oxygen Saturation (SpO₂)/Fraction of Inspired Oxygen (FiO₂) Ratio Time at Risk and Hospital Mortality in Mechanically Ventilated Patients', *The Permanente journal*, vol. 24, p. 19.113.
- Briel, M, Meade, M, Mercat, A, Brower, RG, Talmor, D, Walter, SD, Slutsky, AS, Pullenayegum, E, Zhou, Q, Cook, D, Brochard, L, Richard, J-CM, Lamontagne, F, Bhatnagar, N, Stewart, TE & Guyatt, G 2010, 'Higher vs Lower Positive End-Expiratory Pressure in Patients With Acute Lung Injury and Acute Respiratory Distress Syndrome: Systematic Review and Meta-analysis', *JAMA*, vol. 303, no. 9, pp. 865-873.
- Carney, D, DiRocco, J & Nieman, G 2005, 'Dynamic alveolar mechanics and ventilator-induced lung injury', *Crit Care Med*, vol. 33, no. 3, pp. S122-S128.
- Cereda, M, Emami, K, Xin, Y, Kadlecsek, S, Kuzma, NN, Mongkolwisetwara, P, Profka, H, Pickup, S, Ishii, M, Kavanagh, BP, Deutschman, CS & Rizi, RR 2013, 'Imaging the interaction of atelectasis and overdistension in surfactant-depleted lungs', *Critical care medicine*, vol. 41, no. 2, pp. 527-535.
- Chase, JG, Preiser, J-C, Dickson, JL, Pironet, A, Chiew, YS, Pretty, CG, Shaw, GM, Benyo, B, Moeller, K, Safaei, S, Tawhai, M, Hunter, P & Desaive, T 2018, 'Next-generation, personalised, model-based critical care medicine: a state-of-the art review of in silico virtual patient models, methods, and cohorts, and how to validate them', *BioMedical Engineering OnLine*, vol. 17, no. 1, p. 24.
- Chiew, YS, Chase, JG, Shaw, GM, Sundaresan, A & Desaive, T 2011, 'Model-based PEEP optimisation in mechanical ventilation', *BioMedical Engineering OnLine*, vol. 10, no. 1, p. 111.
- Damanhuri, NS, Chiew, YS, Othman, NA, Docherty, PD, Pretty, CG, Shaw, GM, Desaive, T & Chase, JG 2016, 'Assessing respiratory mechanics using pressure reconstruction method in mechanically ventilated spontaneous breathing patient', *Comput Methods Programs Biomed*, vol. 130, pp. 175-185.
- Fisher, JB, Mammel, MC, Coleman, JM, Bing, DR & Boros, SJ 1988, 'Identifying lung overdistention during mechanical ventilation by using volume-pressure loops', *Pediatric Pulmonology*, vol. 5, no. 1, pp. 10-14.
- Force*, TADT 2012, 'Acute Respiratory Distress Syndrome: The Berlin Definition', *JAMA*, vol. 307, no. 23, pp. 2526-2533.

- Fumagalli, J, Santiago, RRS, Teggia Droghi, M, Zhang, C, Fintelmann, FJ, Troschel, FM, Morais, CCA, Amato, MBP, Kacmarek, RM, Berra, L & Investigators, obotLRT 2019, 'Lung Recruitment in Obese Patients with Acute Respiratory Distress Syndrome', *Anesthesiology*, vol. 130, no. 5, pp. 791-803.
- Galiatsou, E, Kostanti, E, Svama, E, Kitsakos, A, Koulouras, V, Efremidis, SC & Nakos, G 2006, 'Prone Position Augments Recruitment and Prevents Alveolar Overinflation in Acute Lung Injury', *American Journal of Respiratory and Critical Care Medicine*, vol. 174, no. 2, pp. 187-197.
- Gomez-Laberge, C, Arnold, JH & Wolf, GK 2012, 'A Unified Approach for EIT Imaging of Regional Overdistension and Atelectasis in Acute Lung Injury', *IEEE Transactions on Medical Imaging*, vol. 31, no. 3, pp. 834-842.
- Jonson, B, Richard, J-C, Straus, C, Mancebo, J, Lemaire, F & Brochard, L 1999, 'Pressure-Volume Curves and Compliance in Acute Lung Injury', *American Journal of Respiratory and Critical Care Medicine*, vol. 159, no. 4, pp. 1172-1178.
- Kárason, S, Søndergaard, S, Lundin, S & Stenqvist, O 2001, 'Continuous on-line measurements of respiratory system, lung and chest wall mechanics during mechanic ventilation', *Intensive Care Medicine*, vol. 27, no. 8, pp. 1328-1339.
- Kim, KT, Morton, S, Howe, S, Chiew, YS, Knopp, JL, Docherty, P, Pretty, C, Desaive, T, Benyo, B & Szlavecz, A 2020, 'Model-based PEEP titration versus standard practice in mechanical ventilation: a randomised controlled trial', *Trials*, vol. 21, no. 1, p. 130.
- Langdon, R, Docherty, PD, Mansell, EJ & Chase, JG 2018, 'Accurate and precise prediction of insulin sensitivity variance in critically ill patients', *Biomedical Signal Processing and Control*, vol. 39, pp. 327-335.
- Laufer, B, Docherty, PD, Knörzer, A, Chiew, YS, Langdon, R, Möller, K & Chase, JG 2017, 'Performance of variations of the dynamic elastance model in lung mechanics', *Control Engineering Practice*, vol. 58, pp. 262-267.
- Maggiore, SM, Richard, JC & Brochard, L 2003, 'What has been learnt from P/V curves in patients with acute lung injury/acute respiratory distress syndrome', *Eur Respir J*, vol. 22, no. 42_suppl, pp. 22s-26.
- Morton, SE, Dickson, J, Chase, JG, Docherty, P, Desaive, T, Howe, SL, Shaw, GM & Tawhai, M 2018, 'A virtual patient model for mechanical ventilation', *Comput Methods Programs Biomed*, vol. 165, pp. 77-87.
- Morton, SE, Knopp, JL, Chase, JG, Docherty, P, Howe, SL, Möller, K, Shaw, GM & Tawhai, M 2019a, 'Optimising mechanical ventilation through model-based methods and automation', *Annual Reviews in Control*, vol. 48, pp. 369-382.
- Morton, SE, Knopp, JL, Chase, JG, Möller, K, Docherty, P, Shaw, GM & Tawhai, M 2019b, 'Predictive Virtual Patient Modelling of Mechanical Ventilation: Impact of Recruitment Function', *Annals of Biomedical Engineering*, vol. 47, no. 7, pp. 1626-1641.
- Morton, SE, Knopp, JL, Tawhai, MH, Docherty, P, Heines, SJ, Bergmans, DC, Möller, K & Chase, JG 2020, 'Prediction of lung mechanics throughout recruitment maneuvers in pressure-controlled ventilation', *Computer Methods and Programs in Biomedicine*, vol. 197, p. 105696.
- Pavone, L, Albert, S, DiRocco, J, Gatto, L & Nieman, G 2007, 'Alveolar instability caused by mechanical ventilation initially damages the nondependent normal lung', *Critical Care*, vol. 11, no. 5, p. R104.
- Stahl, CA, Möller, K, Schumann, S, Kuhlen, R, Sydow, M, Putensen, C & Guttman, J 2006, 'Dynamic versus static respiratory mechanics in acute lung injury and acute respiratory distress syndrome', *Crit Care Med*, vol. 34, no. 8, pp. 2090-2098.
- Stenqvist, O & Odenstedt, H 2007, 'Alveolar Pressure/volume Curves Reflect Regional Lung Mechanics', *Intensive Care Medicine*, pp. 407-414.
- Sun, Q, Zhou, C & Chase, JG 2020, 'Parameter updating of a patient-specific lung mechanics model for optimising mechanical ventilation', *Biomedical Signal Processing and Control*, vol. 60, p. 102003.
- Sundaresan, A & Chase, JG 2012, 'Positive end expiratory pressure in patients with acute respiratory distress syndrome – The past, present and future', *Biomedical Signal Processing and Control*, vol. 7, no. 2, pp. 93-103.
- Sundaresan, A, Chase, JG, Shaw, GM, Chiew, YS & Desaive, T 2011, 'Model-based optimal PEEP in mechanically ventilated ARDS patients in the Intensive Care Unit', *BioMedical Engineering OnLine*, vol. 10, no. 1, p. 64.
- The ARDS Definition Task Force 2012, 'Acute respiratory distress syndrome: The berlin definition', *JAMA: The Journal of the American Medical Association*, vol. 307, no. 23, pp. 2526-2533.
- Vieira, SRR, Puybasset, L, Richecoeur, J, Lu, QIN, Cluzel, P, Gusman, PB, Coriat, P & Rouby, J-J 1998, 'A Lung Computed Tomographic Assessment of Positive End-Expiratory Pressure-induced Lung Overdistension', *American Journal of Respiratory and Critical Care Medicine*, vol. 158, no. 5, pp. 1571-1577.
- Zhou, C & Chase, JG 2020, 'A new pinched nonlinear hysteretic structural model for automated creation of digital clones in structural health monitoring', *Structural Health Monitoring*
- Zhou, C, Chase, JG, Knopp, J, Sun, Q, Tawhai, M, Möller, K, Heines, SJ, Bergmans, DC, Shaw, GM & Desaive, T 2021, 'Virtual patients for mechanical ventilation in the intensive care unit', *Computer Methods and Programs in Biomedicine*, vol. 199, p. 105912.
- Zhou, C, Chase, JG, Rodgers, GW, Tomlinson, H & Xu, C 2015, 'Physical Parameter Identification of Structural Systems with Hysteretic Pinching', *Computer-Aided Civil and Infrastructure Engineering*, vol. 30, no. 4, pp. 247-262.